

Sensitivity and Antenna Noise Temperature Analysis of the Feed System for the Onsala Twin Telescopes

J. Flygare, M. Pantaleev, B. Billade, M. Dahlgren, L. Helldner, R. Haas

Abstract The demand for higher precision measurements in Very Long Baseline Interferometry (VLBI) continues to grow, which drives the technical development of next generation international VLBI stations called the VLBI Global Observing System (VGOS). The VGOS design includes the idea of twin telescopes, i.e. two identical telescopes that will be used for continuous observations to study geodynamical processes. Such a twin telescope system has recently been installed at the Onsala Space Observatory, Sweden. The Onsala twin telescopes (OTT) are 13.2 m diameter, dual-reflector systems with a ring-focus sub-reflector. In this paper we present the estimated performance, focusing on the achievable system equivalent flux density (*SEFD*), sky noise modeling, and antenna noise temperature. We evaluate the system for two different cryogenic wideband quad-ridge flared horn (QRFH) feed setups operating over 3 – 18 GHz and 4.6 – 24 GHz. Analysis based on measured feed data shows a low antenna noise temperature and that *SEFD* of 1000 Jy can be achieved for the system. The result from Y-factor test shows $T_{\text{REC}} = 10$ K over most of the frequency band.

Keywords Very Long Baseline Interferometry (VLBI), VLBI Global Observing System (VGOS), Wideband, Feed, System Equivalent Flux Density (*SEFD*), Quad-Ridge Flared Horn (QRFH)

1 Introduction

The technique of Geodetic Very Long Baseline Interferometry (Geo-VLBI) is well established as a high preci-



Fig. 1: The Onsala twin telescopes, OTT-North on the left and OTT-South to the right.

sion technique to determine geodetic and geodynamic parameters. It is used extensively to give accurate time estimation and reference frames for the earth's global coordinate systems. Since the first VLBI development in the 1970's and until now, the position accuracy has increased with a factor of 10^3 . The VLBI Global Observing System (VGOS) is the latest step in the realization of this improvement with a goal of a position accuracy of 1 mm. As pointed out in [Schönberger et al. \(2015\)](#), the twin telescope concept is advantageous for several reasons, and due to the short distance between the identical telescopes the difference in atmospheric conditions should be minimal. In 2013 the first twin telescopes were installed at Wettzell Geodetic Observatory, Germany and currently the construction is ongoing for the Ny-Ålesund Geodetic Observatory in Svalbard, Norway. The Onsala twin telescopes (OTT) are the newest addition to the VGOS project, and can be seen in [Fig. 1](#). The telescopes were inaugurated with great celebrations on the 18th of May, 2017.

In this paper we focus on the sensitivity performance of the OTT based on measured data. The Figure-of-Merit (FoM), the system equivalent flux

Jonas Flygare · Miroslav Pantaleev · Bhushan Billade · Magnus Dahlgren, Leif Helldner · Rüdiger Haas
Onsala Space Observatory, Department of Space, Earth and Environment, Chalmers University of Technology, SE-439 92 Onsala, Sweden
Email: jonas.flygare@chalmers.se

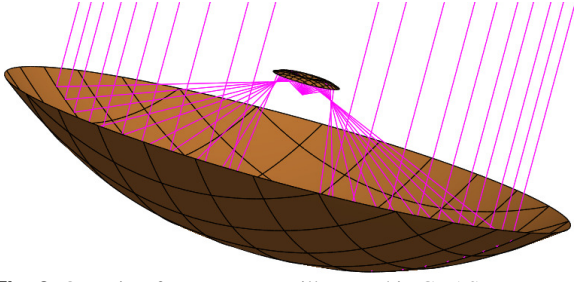


Fig. 2: OTT ring-focus geometry illustrated in GRASP.

density ($SEFD$), is specified to be below 2100 Jy for 3 – 18 GHz and elevations down to 30° above the horizon. In Eq. 1 it can be seen that for a given incoming flux density, S_{in} , the Signal-to-Noise Ratio (SNR) increases with a decreasing $SEFD$,

$$SNR = \frac{S_{in}}{SEFD} \sqrt{t \cdot f_{BW}}, \quad (1)$$

where t is the integration time and f_{BW} is the bandwidth. Therefore, minimizing $SEFD$ as much as possible translates to high sensitivity and shorter integration time for observations. $SEFD$ is proportional to the ratio of total system noise temperature, T_{sys} , over effective collecting area of the telescope, A_{eff} , according to Eq. 2,

$$SEFD = \frac{2k_B T_{sys}}{A_{eff}}, \quad (2)$$

where k_B is the Boltzmann constant. The effective area of the telescope is defined as $A_{eff} = \eta_a A_{phy}$ where η_a is the aperture efficiency and A_{phy} is the physical collecting area of the dish. Total system noise temperature is defined as $T_{sys} = T_A + T_{REC}$, where T_A is the antenna noise temperature and T_{REC} is the receiver noise temperature including mismatches, feed ohmic losses and the noise temperature of the cryogenic Low-Noise Amplifiers (LNA). In Sec. 3 we discuss T_A more and the modeling of the sky noise temperature and spill-over calculation.

2 Telescope geometry

The OTT dish geometry is of ring-focus dual-reflector type with a $D = 13.2$ m and a half-subtended angle $\theta_0 = 65^\circ$ and was designed and delivered by MT Mechatronics (MTM). A simplified picture of the ring-focus geometry is shown in Fig. 2 with a 1.5 m on-axis sub-reflector. This geometry results in a telescope focus close to the sub-reflector and not at the main-reflector apex, therefore no rays are reflecting from the center hole of the main-reflector. Rays from the main-reflector outer rim reflect into boresight of the feed and rays from

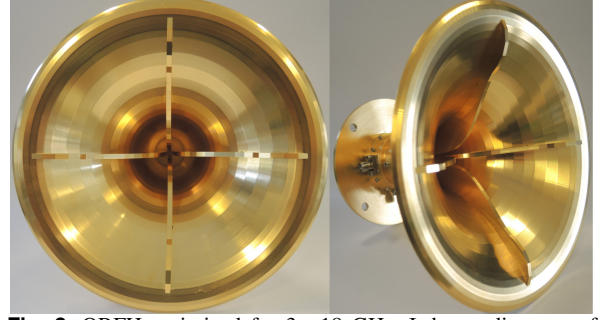


Fig. 3: QRFH optimized for 3 – 18 GHz. It has a diameter of 148 mm and a length of 102 mm.

close to the center hole reflect at the sub-reflector outer rim into the feed. This construction results in a higher aperture efficiency compared to common unshaped dual-reflector systems (Milligan, 2005). The subtended angle is suitable for linearly dual-polarized broadband feeds such as the quad-ridge flared horn (QRFH) (Akgiray et al., 2011) and the Eleven Feed (Yang et al., 2011). The ring-focus antenna geometry makes the system sensitive for horizontal radio frequency interference (RFI) due to the sub-reflector shape, and depending on the local situation a broadband feed with a strict cut-off above the lowest part of the S-band could be needed (Schüler et al., 2015), which is an inherent feature of the QRFH. Both the QRFH and the Eleven Feed are very well known technologies and have been studied thoroughly for the VGOS project. These feed concepts give near-constant beamwidth, ultra-wideband frequency performance and a compact footprint. The Eleven Feed has a constant phase center location and QRFH can be easily fed with one single-ended LNA per polarization. The receiver system and cryogenic dewar was designed so that it could house either of the feed concepts and be interchangeable.

3 Noise temperature modeling

To calculate the $SEFD$ we need to accurately estimate the antenna noise temperature, T_A . This was done using a complete system simulator, provided by Marianna Ivashina at the antenna group at Chalmers University of Technology (Ivashina et al., 2011). The software combines the feed beam patterns with the dish geometry and calculates the full beam pattern of the telescope through physical optics (PO) and physical theory of diffraction (PTD) in the GRASP software. Then, by integrating the noise temperature distribution, $T(\theta, \phi, f)$, of the sky (Fig. 5) and ground over all angles weighted with the beam pattern according to Eq. 3,

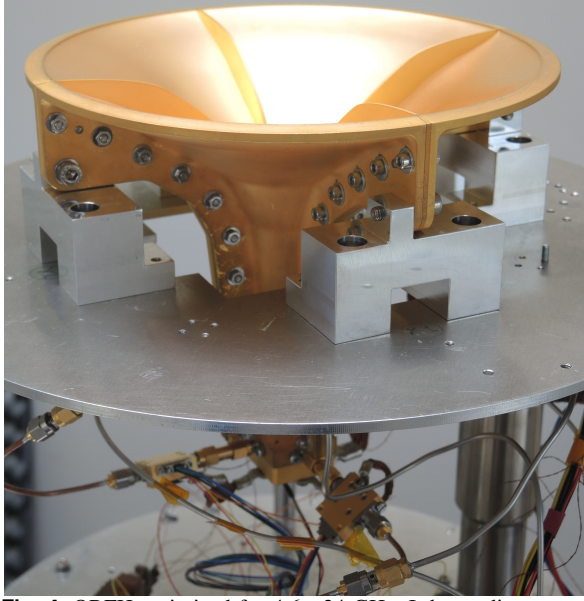


Fig. 4: QRFH optimized for 4.6 – 24 GHz. It has a diameter of 202 mm and a length of 182 mm. The feed is shown mounted inside the dewar for test with the LNAs visible at the bottom.

$$T_A = \frac{\iint_{4\pi} G(\theta, \phi, f) T(\theta, \phi, f) \sin \theta d\theta d\phi}{\iint_{4\pi} G(\theta, \phi, f) \sin \theta d\theta d\phi} \quad (3)$$

we can estimate the antenna noise temperature T_A . In this calculation $G(\theta, \phi, f)$ is the beam pattern of the telescope, θ is elevation, ϕ azimuth and f is frequency. The significant contributions to the antenna noise are the sky-noise from the main beam and the spill-over terminated on the ground ($T_g = 290$ K). The noise distribution for the full sphere surrounding the telescope is given according to Eq. 4,

$$T(\theta, \phi, f) = \begin{cases} T_s(\theta, \phi, f) & 90^\circ \geq |\theta| > 0^\circ \\ T_g & 0^\circ \geq |\theta| \geq -90^\circ \end{cases} \quad (4)$$

From the noise temperature calculations together with the aperture efficiency, we can accurately estimate the *SEFD* of the complete telescope system. For clarification, a schematic over the system simulator process is shown in Fig. 6.

4 Feed system performance

In this section we show the performance of a 3 – 18 GHz QRFH, see Fig. 3, estimated on the OTT with measured feed beam patterns. The feed was optimized and

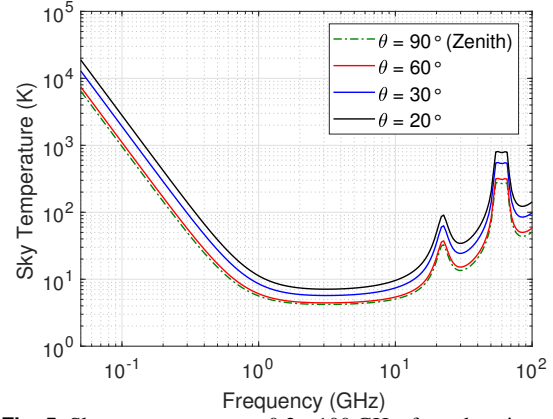


Fig. 5: Sky temperature over 0.2 – 100 GHz, four elevations.

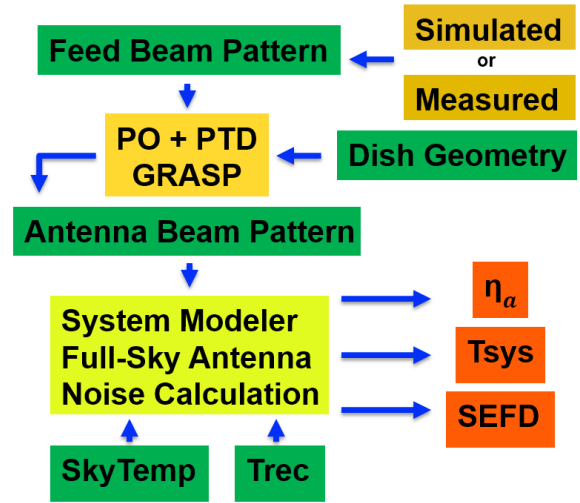


Fig. 6: Schematic of the steps in the system simulator illustrating the full calculation procedure.

delivered by the California Institute of Technology, Pasadena, CA, USA, for these frequencies. We also show the performance of a QRFH over 4.6 – 24 GHz, see Fig. 4, designed at Onsala and the antenna group at Chalmers for a different project (Dong et al., 2017) and how it could be a possible upgrade in the future for OTT. T_{REC} was measured at Onsala for both receiver systems using the standard Y-factor method with a hot (absorber) and cold (sky) load. The systems includes cryogenic low-noise amplifiers (LNA) supplied by the company Low Noise Factory (LNF) based in Gothenburg, Sweden. Antenna noise temperature was calculated using measured feed beam patterns in the system simulator described in Sec. 3.

Aperture efficiency for the 3 – 18 GHz QRFH (6 : 1 bandwidth) is above 50 % across the band with an average of 58 %, see Fig. 7. This is slightly below the expected 60 % and most likely depends on ridge misalignment in the feed during the assembly. The 4.6 – 24 GHz

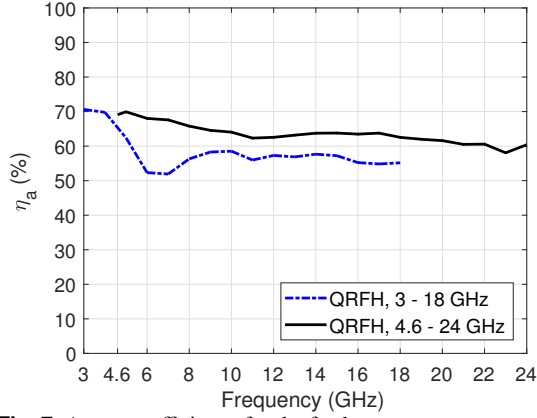


Fig. 7: Aperture efficiency for the feed systems.

QRFH (5.2 : 1 bandwidth) shows high and constant aperture efficiency above 60 % across almost the entire band with an average of 63 %.

Both feeds show similar performance in antenna noise, $T_A = 10$ K in zenith elevation, for the overlapping frequencies. The 4.6–24 GHz QRFH show slightly better performance due to higher spill-over efficiency, see Fig. 8. The difference in T_A between the feeds for lower elevation means that a bigger fraction of the side-lobes are terminated on the ground for the 3–18 GHz feed at this range of elevation. At the upper end of the frequency band in Fig. 8 we see an increase in sky-noise from the water-vapor line at 22.2 GHz which is an unavoidable feature of the surrounding sky temperature, see Fig. 5. The receiver noise of both systems is measured to excellent $T_{\text{REC}} = 10$ K over most of the frequency band, see Fig. 9. Total system noise temperature for each of the two systems, T_{sys} , are between 20–25 K over most of the bands for zenith elevation and 10 K higher for the lower elevation $|\theta| = 30^\circ$. In both systems we add another 2 K to the total system noise accounting for back-end noise contribution. According to Eq. 2 this results in $SEFD = 1000$ Jy, clearly fulfilling the requirement of lower than 2100 Jy over the 3–18 GHz band, see Fig. 10. For the frequency range 21–24 GHz, $SEFD$ is degraded due to the very strong absorption in the water-vapor line and can not be expected to achieve the same performance as the rest of the band.

5 Conclusions

Through full system antenna noise analysis, the OTT feed systems show $SEFD = 1000$ Jy over most of the 3–18 GHz and all elevations. This is clearly fulfilling the specification of maximum 2100 Jy allowed. Both QRFH systems presented here show excellent $T_{\text{REC}} =$

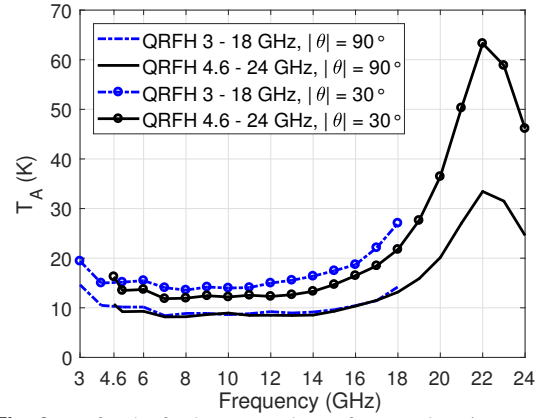


Fig. 8: T_A for the feed systems shown for two elevations.

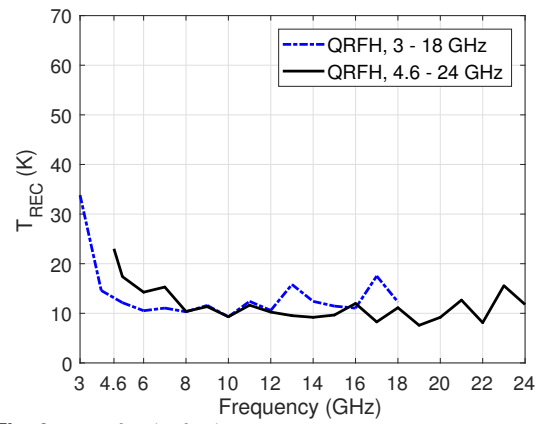


Fig. 9: T_{REC} for the feed systems.

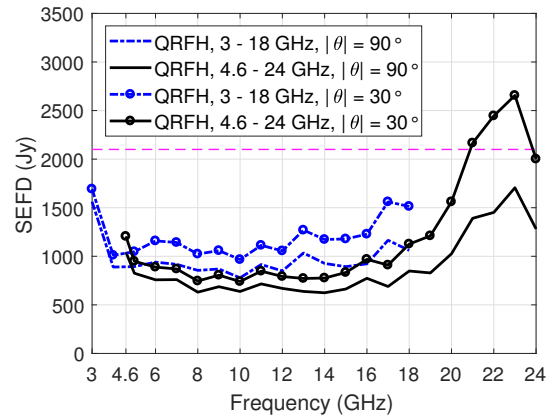


Fig. 10: $SEFD$ for the feed systems shown for two elevations. The dashed purple line shows the maximum allowed $SEFD$ over 3–18 GHz.

10 K and should be considered as good candidates for operation. The OTT is indeed a high-end VGOS system that will contribute substantially to next generation of Geo-VLBI research.

Acknowledgement

The authors would like to thank Sander Weinreb at Caltech for providing us with the QRFH feed design for 3 – 18 GHz. We would like to thank Jian Yang from the Antenna Group at Chalmers University of Technology, Sweden and Bin Dong from National Astronomical Observatories, Chinese Academy of Sciences, China for the development and design of the 4.6 – 24 GHz QRFH and assisting with beam pattern measurements. We would also like to thank José Manuel Serna Puente, José Antonio López Fernández and Samuel López Ruiz at Observatorio de Yebes, Spain for beam pattern measurements. The authors would also like to thank Peter Forkman at Onsala for supplying an accurate sky model for the Y-factor measurements.

References

- Akgiray A, Weinreb S, Imbriale W (2011) Design and measurements of dual-polarized wideband constant-beamwidth quadruple-ridged flared horn. *Proc. IEEE Antennas Propag. Soc. Int. Symp. (APSURSI2011)*, 1135–1138.
- Dong B, Yang J, Dahlström J, Flygare J, Pantaleev M, Billade B (2017). Optimization and Realization of Quadruple-ridge Flared Horn with New Spline-defined Profiles as a High-efficiency Feed for Reflectors over 4.6–24 GHz. submitted to *IEEE Trans. Antennas. Propag.*
- Ivashina M, Iupikov O, Maaskant R, van Cappellen W, Oosterloo T (2011) An optimal beamforming strategy for wide-field surveys with phased-array-fed reflector antennas. *IEEE Trans. Antennas. Propag.*, 59(6), 1864–1875.
- Milligan T A (2005) Modern Antenna Design. 2nd Edition. NJ, USA: Wiley-IEEE Press.
- Schönberger C, Gnisen P, Böhm J, Haas R (2015) Twin Telescopes at Onsala and Wettzell and their contribution to the VGOS System. In: R. Haas, F. Colomer (eds.), *Proc. 22nd European VLBI Group for Geodesy and Astrometry Working Meeting*, 120–124.
- Schüler T, Kronschnabl G, Plötz C, Neidhardt A, Bertarini A, Bernhart S, Nothnagel A (2015) Initial Results Obtained with the First TWIN VLBI Radio Telescope at the Geodetic Observatory Wettzell. *Sensors*, 15(8), 18767–18800.
- Yang J, M. Pantaleev M, Kildal P-S, Klein B, Karandikar Y, Helldner L, Wadefalk N, Beaudoin C (2011) Cryogenic 2-13 GHz Eleven Feed for Reflector Antennas in Future Wideband Radio Telescopes. *IEEE Trans. Antennas. Propag.*, 59(6), 1918–1934.